FEBS Letters 583 (2009) 2887–2892

FEBS Letters

journal homepage: www.FEBSLetters.org

Kinetic and thermodynamic properties of the folding and assembly of formate dehydrogenase

Emel B. Ordu [a,b,c], Gus Cameron [d], Anthony R. Clarke [d], Nevin Gül Karagüler [a,b,*]

[a] Istanbul Technical University, Faculty of Science and Letters, Department of Molecular Biology and Genetics, Istanbul, Turkey
[b] Istanbul Technical University, Molecular Biology-Biotechnology and Genetics Research Centre, 34469 Istanbul, Turkey
[c] Yildiz Technical University, Faculty of Science and Letters, Department of Biology, Davutpasa, 34220 Esenler, Istanbul, Turkey
[d] University of Bristol, Department of Biochemistry, Bristol BS8 1TD, Avon, England

ARTICLE INFO

Article history:
Received 6 May 2009
Revised 18 July 2009
Accepted 26 July 2009
Available online 3 August 2009

Edited by Miguel De la Rosa

Keyword:
Assembly mechanism
Folding mechanism
Formate dehydrogenase
Candida methylica

ABSTRACT

The folding mechanism and stability of dimeric formate dehydrogenase from *Candida methylica* was analysed by exposure to denaturing agents and to heat. Equilibrium denaturation data yielded a dissociation constant of about 10^{-13} M for assembly of the protein from unfolded chains and the kinetics of refolding and unfolding revealed that the overall process comprises two steps. In the first step a marginally stable folded monomeric state is formed at a rate (k_1) of about 2×10^{-3} s^{-1} (by deduction k_{-1} is about10^{-4} s^{-1}) and assembles into the active dimeric state with a bimolecular rate constant (k_2) of about 2×10^4 M^{-1} s^{-1}. The rate of dissociation of the dimeric state in physiological conditions is extremely slow ($k_{-2} \sim 3 \times 10^{-7}$ s^{-1}).

1. Introduction

It is arguable that efforts to control the stability of proteins by genetic modification of sequence could be laid on a firmer foundation such that we would understand better the full mechanism of folding and unfolding of the active system. This, ideally, requires elucidation of the kinetic and equilibrium properties of each step and, in addition, it would be illuminating to know the temperature-dependence of the system so that its classical thermodynamic properties can be derived. With such a foundation, it might be possible to target certain critical steps in the process, so that sequence engineering would be more rationally directed.

While there is a wealth of data on the kinetics and thermodynamics of folding in single-chain proteins [1], our understanding of folding and assembly processes in multi-chain proteins is less comprehensive. Clearly, it is more demanding to study such systems, owing to their greater complexity and the frequently encountered inefficiency of self-assembly of oligomeric structures. However, many of the proteins of interest in biotechnology are oligomeric, as are many of the structures in biological systems where we want to understand the dynamics of assembly and disassembly and for these reasons it is useful to examine such mechanisms with a view to providing a framework for their analysis.

In this paper we use *Candida methylica* formate dehydrogenase (*cm*FDH) cloned and overproduced by Allen and Holbrook [2] as a study object owing to its practical potential in synthetic chemistry and the ease of measuring its regain of activity. The native form of *cm*FDH is a dimer and each subunit has 364 residues folded into two distinct but structurally homologous domains, each comprising a parallel β-sheet core surrounded by α-helices arranged in a Rossmann-type fold. One domain is functionally defined by coenzyme binding, the other by possessing the residues necessary for catalysis; coenzyme and substrate are encapsulated in the inter-domain cleft during the catalytic reaction. The molecule dimerizes by twofold symmetrical interactions between the coenzyme-binding domains while the catalytic domains are distal to the dimer interface [3].

FDH catalyses the conversion of formate and NAD^+ to carbon dioxide and NADH and thus has considerable potential in enzymatic synthesis. Its usefulness lies in the fact that it is capable of regenerating NADH in enzymatic reductions of aldehydes and ketones to form chirally pure alcohols that are valuable as building blocks in the synthesis of more elaborate structures [4]. While

Abbreviations: *cm*FDH, *Candida metylica* formate dehydrogenase; NAD, nicotinamide adenine dinucleotide; yTIM, yeast triosephosphate isomerase; apo-SOD, apo-superoxide dismutase; N-PGK, N-domain of phosphoglycerate kinase

* Corresponding author. Address: Istanbul Technical University, Faculty of Science and Letters, Department of Molecular Biology and Genetics, 34469 Istanbul, Turkey. Fax: +90 212 2856386.
E-mail address: karaguler@itu.edu.tr (N.G. Karagüler).

0014-5793/$36.00
doi:10.1016/j.febslet.2009.07.048

there has been much empirical work on stabilizing FDHs against elevated temperatures and other environmental factors such as oxidation [5], the thermodynamic and kinetic properties of its folding and unfolding pathway have not been dissected in detail. In this paper, we define the rates of steps in the minimal model of folding and assembly reaction and deduce the equilibrium properties of the system with respect to its thermal and denaturant sensitivities. These results should act as a basis for understanding the effects of site-specific engineering or forced evolution on the stability of this molecule.

2. Materials and methods

2.1. Protein purification

Wild-type *cm*FDH was prepared and purified as described previously [6]. SDS–PAGE and Coomassie Brilliant Blue staining showed the protein to be >95% pure after purification. Protein concentration was estimated at 280 nm from its specific extinction coefficient, 49 170 cm^{-1} M^{-1}, and expressed in terms of the monomeric protein concentration using monomer mass of 42 000 Da.

2.2. Equilibrium unfolding assay of cmFDH

Unfolding experiments were performed by using 0.1 and 1 μM protein. Protein samples were incubated in 20 mM Tris, pH 8 at a series of GdnHCl concentrations at 25 °C in previous experiments. According to results of preliminary experiments unfolding studies were carried on with 0.1 μM protein, samples were incubated at different temperatures (25, 30, 35, 40, 45 °C) for 4 h. The protein fluorescence intensity of each sample was measured between 300 and 400 nm using an excitation wavelength of 285 nm in a Spex Fluoromax spectrofluorometer. Maximum emission was obtained at 350 nm. For each sample three scans were averaged for final spectrum. Denaturation curves were analysed by assuming a two-state mechanism. Data were fitted Eq. (1) to calculate K_w by fixing the m at the mean value for all transitions with Grafit 5.

$$K = K_w \cdot \exp(m \cdot D) \tag{1}$$

$$a = 1$$
$$b = -(2 + 1/(2 \cdot K \cdot Mo))$$
$$c = 1$$
$$\text{alpha}_D = (-b - (b^2 - 4 * a * c)^{0.5})/(2 * a)$$
$$Y = \text{sig}_D \cdot \text{alpha}_D + \text{sig}_M \cdot (1 - \text{alpha}_D)$$

where K_w is the D/M in water, sig_D is the signal for folded state, sig_M is the signal for unfolded state and Mo is the monomer concentration as a constant. For the analysis of equilibrium data, guanidinium hydrochloride concentration ([GdnHCl]) is converted to molar denaturant activity (D), according to the following relationship:

$D = ([\text{GdnHCl}] \cdot C_{0.5})/([\text{GdnHCl}] + C_{0.5})$, where $C_{0.5}$ is a denaturation constant with a value of 7.5 M [7].

The change in free energy between the folded and unfolded states in the absence of denaturant, ΔG_w, was calculated for each temperature (25, 30, 35, 40, 45 °C), using the $\Delta G = -RT \ln K_w$ relationship. For the free-energy change associated with a particular transition with temperature, data were fitted to the following equation:

$$\Delta G = \Delta H + \Delta C_p \cdot (T - T_o) - T \cdot \Delta S - \Delta C_p \cdot T \cdot \ln(T/T_o), \tag{2}$$

where $\Delta H(T_o)$, $\Delta S(T_o)$ and ΔC_p are the enthalpy, entropy and heat capacity changes, respectively, at a defined reference temperature (T_o). All data were fitted using the Grafit 5 analysis software (Erithracus Software, UK).

2.3. Stopped flow unfolding experiments of cmFDH

The rate constant for unfolding at a particular concentration of GdnHCl was measured using stopped flow fluorometer (Applied Photophysics (05-109) pbp Spectra Kinetic Monochromator). One micromolar protein is jumped into 4, 4.5, 5, 5.5 and 6 M GdnHCl concentrations and fluorescence decay was measured against time. Protein was excited by monochromatic light at 285 nm and the resulting fluorescence was selected with a WG320 cut-off filter. Each recorded transient was an average of at least three individual reactions. Reactions were recorded at 25 °C. Data were fitted to single exponential decay pattern. The rate constants were plotted as a function of denaturant activity to extract the rate constant for unfolding in the absence of denaturant ($k_{u(w)}$) according to the following equation:

$$K_u = k_{u(w)} \cdot \exp(-m \cdot D) \tag{3}$$

2.4. Refolding activity assay

*cm*FDH enzyme was unfolded in the unfolding buffer containing 4 M GdnHCl and 20 mM DTT in 20 mM Tris pH 8, at room temperature for 2 h. Refolding assay was initiated by the dilution of 16.6 μM unfolded FDH to 0.1, 0.2, 0.3, 0.5 and 1 μM concentration in the refolding assay buffer containing 20 mM Tris pH 8, 5 mM DTT, 20 mM formate, 1 mM nicotinamide adenine dinucleotide (NAD). The production of NADH was monitored by following the increase in absorption at 340 nm spectrophotometrically to assess the refolding yield of different concentrations of FDH. Measurements were performed by using UV/VIS Spectrometer Lambda 2 for 60 min in 1 ml cuvette. For numerical analysis of the refolding curves data were globally fitted using a numerical method [8] to the system $2U \rightarrow 2M \rightarrow D$.

2.5. Thermal denaturation

The proteins (wild-type and mutant FDHs) were aliquot and incubated at different temperatures with 2 °C intervals for 20 min as triplicate. Remaining activity measurements were performed at 25 °C in a reaction mixture containing 20 mM Tris Buffer at pH 8, 1 mM NAD^+, 2 mM formate and 0.4 μM enzyme. Rate constants (k) were derived directly from the residual activity (A) by the following relationship:

$$A = A_o \cdot \exp(-k \cdot t_{\text{inc}}) \tag{4}$$

where t_{inc} is the period of incubation (in our case 1200s) and A_o is the initial activity. The free-energy barrier for unfolding as a function of temperature is described by the relationship:

$$k = k_o \cdot \exp(-\Delta G/(R \cdot T)) \tag{5}$$

where $\Delta G = \Delta H + \Delta C_p \cdot (T - T_o) - T \cdot \Delta S - \Delta C_p \cdot T \cdot \ln(T/T_o)$ and k_o is the rate of an unfolding reaction in the absence of an activation barrier (a value of 10^7 s^{-1} was taken for our analysis, see Section 3).

3. Results and discussion

3.1. Equilibrium unfolding

To measure the free energy of folding of this dimeric FDH, we analysed the guanidinium-induced denaturation of the enzyme at equilibrium. Upon unfolding there is a large (~70%) quench is the native tryptophan fluorescence and the transition to the unfolded state occurs in a single step, without intermediates, as shown in Fig. 1. As denaturation of the dimer requires dissociation

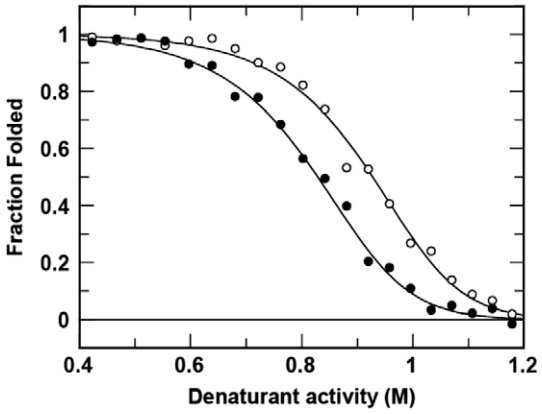

Fig. 1. Equilibrium unfolding curves. Normalized equilibrium unfolding curves of 1 μM (open circles) and 0.1 μM (closed circles) of *cm*FDH. Fluorescence intensity of five tryptophan residue of *cm*FDH was measured at increasing concentrations of the guanidinium hydrochloride ([GdnHCl] at 25 °C. Data were calculated according to equation 1 as a function of GdnHCl denaturant activity. For the 1 μM, $K_w = 1.4$ $(\pm 0.6) \times 10^{13}$ M^{-1}, $m = -17.7 \pm 1.0$ and for the 0.1 μM, $K_w = 1.5$ $(\pm 0.8) \times 10^{13}$ M^{-1}, $m = -17.2 \pm 1.2$. i.e. irrespective of concentration the curves fit with the same parameters.

of the component subunits, this transition must be dependent upon protein concentration. To confirm this we collected equilibrium unfolding curves at two protein concentrations an order of magnitude apart and found that at the higher concentration the midpoint of the curve was shifted to higher concentrations of denaturant (Fig. 1). The data have been fitted to Eq. (1) for dimer dissociation. Owing to the equation accounting for the effect of protein concentration on the denaturation transition, both of the fit-lines produce the same value for the apparent association constant (K_a), i.e. about 10^{13} M^{-1}. Note that this represents the equilibrium: 1 dimer = 2 unfolded monomers, so includes both folding and dissociation processes.

3.2. Thermodynamics of the folding–unfolding transition

The above experiment was performed at a series of temperatures in order to extract the thermal dependence of equilibrium unfolding. The plot in Fig. 2 shows the free-energy change (i.e. $-RT \cdot \ln K_a$) for this transition as a function of temperature fitted to the Gibbs–Helmholtz equation (Eq. (2)). The data shows that, at the reference temperature of 25 °C the enthalpy change on folding (ΔH) is unfavourable (approximately +27 ± 18 kcal/mol), while the entropy change is favourable ($-T\Delta S = -46 \pm 18$ kcal/mol). The heat capacity change (ΔC_p) is -10.5 ± 1.8 kcal/mol/K; a value that is dominated by the degree of desolvation of non-polar surface during the folding process. Hence, ΔC_p is dependent on the chain-length of the protein and can be empirically estimated by the formula [9]:

$$\Delta C_p = N \times -0.015 + 0.13 \text{ kcal/mol/K}$$

The enzyme unfolds in a single transition involving two subunits of 364 residues hence the expected value is −10.8 kcal/mol/K, extremely close to the value of −10.5 derived from the data shown in Fig. 2.

3.3. Kinetics of folding and unfolding

The rate constant for unfolding in the absence of denaturant can be estimated from the data shown in Fig. 3. Extrapolation to zero denaturant yield a value for the rate constant of 3.4 $(\pm 1.5) \times 10^{-7}$ s^{-1} and the Δm-value for the linear free-energy relationship, which relates to the change in solvent exposure between the folded dimeric ground state and the transition state for unfolding, is 4.6 (±) 0.1.

To analyse the folding kinetics, we measured the rate of regain of enzymatic activity from the fully unfolded state as a function of time (Fig. 4). The reactivation curves have a distinct lag phase followed by the acquisition of catalytic activity, showing that refolding process is rate-limited by at least two steps occurring on the same time scale. Further, one of these steps must be multi-molecular since the half-time of refolding is clearly sensitive to the protein concentration. At zero time the tangents to the refolding curves are zero, showing that the intermediate state (or states) lying between the two rate-limiting steps is devoid of activity. In any dimeric system, at least two processes must occur before the individual unfolded chains can form the active state, i.e. folding and association [10]. The simplest model that accounts for the data is an essentially irreversible uni-bi reaction: $2U \rightarrow 2M \rightarrow D$, where U is the unfolded chain, M the folded monomer, and D *is* the active dimer.

Using numerical methods we globally, i.e. simultaneously, fitted the progress curves to the above kinetic model which yielded values of 1.9 $(\pm 0.4) \times 10^{-3}$ s^{-1} for the unimolecular folding step and 1.6 $(\pm 0.5) \times 10^{4}$ M^{-1} s^{-1} for the bimolecular association of

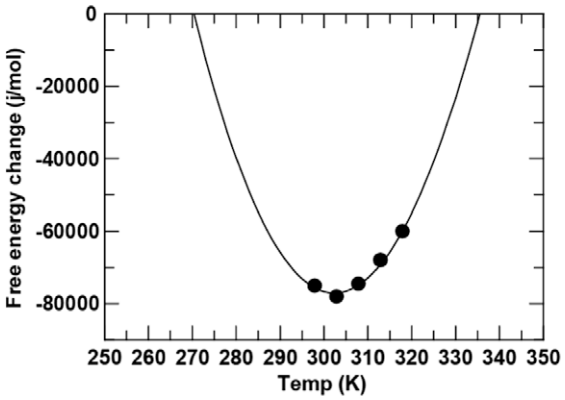

Fig. 2. Thermodynamics of unfolding of *cm*FDH. The free-energy changes of unfolding in water (ΔG_w) over a range of temperatures (T) were determined from equilibrium denaturation data and fitted to Eq. (2), at a reference temperature of $T_o = 298$ K. In this experiments 0.1 μM *cm*FDH protein was used. ΔH, ΔC_p and ΔS values of *cm*FDH were calculated as +27 ± 18 kcal/mol, −10.5 ± 1.8 kcal/mol/K and −46 ± 18 kcal/mol), respectively.

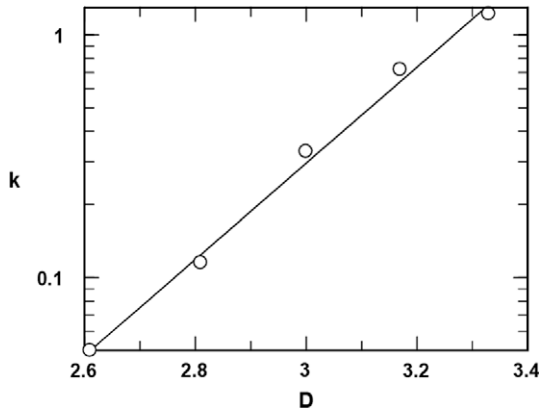

Fig. 3. Unfolding kinetics of *cm*FDH. FDH was unfolded in a stopped flow fluorimeter and the rate constant recorded by analysis of the decrease in fluorescence. The plot shows the variation with denaturant activity fitted to the equation described in Section 2.

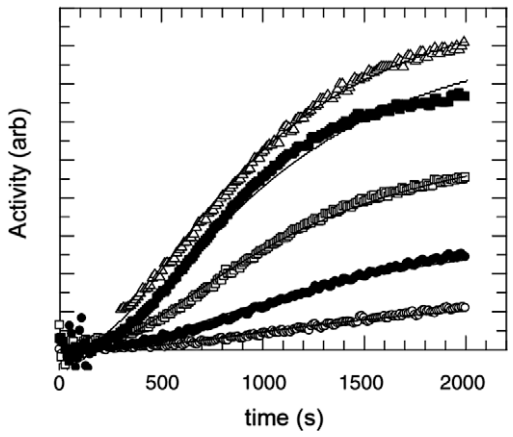

Fig. 4. Refolding of *cm*FDH followed by regain of activity. Activity was measured as a function of time for refolding reactions measured at a series of protein concentrations. The data were globally fitted using a numerical method to the system $2U \rightarrow 2M \rightarrow D$ Fitted rate constants were $1.6 \times 10^{-3}\,s^{-1}$ and $1.9 \times 10^{4}\,M^{-1}\,s^{-1}$.

subunits. Results show a close agreement between model and data over a wide concentration range.

The monomeric intermediate of *cm*FDH forms active dimers at a rate which is slower than expected for a process limited by subunit diffusion in solution. Considerations based on orientational constraints and Brownian diffusion for protein associations have suggested that the basal rate should lie in the range of 10^5–$10^6\,M^{-1}\,s^{-1}$ [11–13]. Electrostatic attractions can enhance this rate significantly, as shown experimentally in the formation of the barnase:barstar complex [14] and the colicin:Im9 interaction [15]. In addition such charge effects have been predicted with reasonable accuracy by models developed by Alsallaq and Zhou [16]. In these studies association rates greater than $10^9\,M^{-1}\,s^{-1}$ were observed, which accords with the value for dimerization of the apo form of superoxide dismutase (see Table 1) where the second-order rate constant is $2 \times 10^9\,M^{-1}\,s^{-1}$. Comparisons with other large proteins that fold through a unimolecular/bimolecular mechanism and for which all steps have been defined are shown in Table 1 [17–20].

At the level of simple reaction kinetics, there are at least three explanations that can account for the apparently slow association rates of the formate dehydrogenase monomers. Firstly, and most straightforwardly, the bimolecular rate might be genuinely $10^4\,M^{-1}\,s^{-1}$ owing to some unusually stringent orientational requirement for securing a productive interaction or owing to charge repulsion between monomers. Secondly, the monomer may be an ensemble of conformations in rapid equilibrium with each other. If only a minority population can dimerize then the apparent bimolecular rate will appear to be slower than the real value. For instance if only 1/10th of the population were competent at any one time, then the apparent second-order rate constant would be 100-fold slower than the real bimolecular constant, i.e. a real rate constant of $10^6\,M^{-1}\,s^{-1}$ would appear to be only $10^4\,M^{-1}\,s^{-1}$. Thirdly, and least intuitively, an unstable dimeric state might be formed with a rapid bimolecular constant, but be unstable at the experimentally accessible concentration of subunits. If there is a rate-limiting unimolecular isomerization of this encounter complex to form the active dimer, then the progress curve will appear second-order because of the depletion of monomers as the reaction progresses. For instance, if the bimolecular rate constant were $10^6\,M^{-1}\,s^{-1}$ and the dissociation rate $10^1\,s^{-1}$, the K_d for this rapid equilibrium would be 10^{-5} M. With a unimolecular rate constant for isomerization of $10^{-1}\,s^{-1}$ and a concentration of 10^{-6} M monomer (i.e. the proportion of dimer in the rapid equilibrium is 1/10th), then the renaturation reaction would be closely approximate to a second-order process with an apparent bimolecular rate constant of $10^4\,M^{-1}\,s^{-1}$.

The relatively slow bimolecular rate constant is combined with a slow rate of dissociation to yield a high stability for the native dimer ($\Delta G^o = -14.6$ kcal/mol), in keeping with other dimeric proteins of high molecular weight. This level of stability ($K_d \sim 10^{-13}$ M) means that at a micromolar concentration, less than one millionth of the enzyme is in the inactive and unstable monomeric state. It is interesting to note that the rate constant for FDH dissociation (Fig. 3) is so slow that, once formed, the dimer has a dissociative half-life of one and a half years.

3.4. Construction of a quantitative mechanism

For the simplest model there are two steps; a unimolecular folding process defined by k_1 and k_{-1} in the forward ($U \rightarrow M$) and reverse direction respectively and a bimolecular process defined by k_2 and k_{-2}. The overall equilibrium constant K_a defines the distribution D/U^2, hence is the product of the two steps. However, since it requires two unfolded chains to form the dimer then:

$$K_a = (k_1/k_{-1})^2 \cdot k_2/k_{-2} \tag{6}$$

Making the assumption that the rate-limiting step in denaturation is dissociation (k_{-2}) then the only value in this system that is not experimentally defined is k_{-1}. This value can be deduced as follows:

$$k_{-1} = ((k_1^2 \cdot k_2)/(K_a \cdot k_{-2}))^{0.5} \tag{7}$$

Given values of $1.5 \times 10^{13}\,M^{-1}$ for K_a, $1.9 \times 10^{-3}\,s^{-1}$ for k_1, $1.6 \times 10^4\,M^{-1}\,s^{-1}$ for k_2 and $3.4 \times 10^{-7}\,s^{-1}$ for k_{-2}, this relationship provides a value for the $M \rightarrow U$ step of about $1 \times 10^{-4}\,s^{-1}$. In this system M has no enzymatic activity and its stability is marginal, the free-energy change for this step being only 1.7 kcal/mol.

3.5. A simplified analytical method for approximating folding and assembly rates

The formal analytical equation for fitting a uni–bi kinetic systems is extremely unwieldy, therefore to extract the values for rate constants in the renaturation reaction we have used numerical fitting procedures. The numerical fitting technique employed to extract the forward rate constants in the renaturation process

Table 1
Comparison equilibrium and kinetic parameters of some large proteins that fold through a unimolecular/bimolecular mechanism.

Protein (residues)	$\Delta G\ U \rightarrow M/\Delta G^o\ M \rightarrow D$ (kcal mol^{-1})	k_f (s^{-1})	k_u (s^{-1})	k_{ass} ($M^{-1}\,s^{-1}$)	k_{dis} (s^{-1})
YbeA (155) [10]	−2.8/−13.3	1.6e−1	8.1e−4	3.9e4	4.3e−4
Yeast triosephosphate isomerase (yTIM) (247) [11]	−4.0/−16.8	1.4e−2	3.6e−6	6.7e5	3.5e−8
apo-superoxide dismutase (apo-SOD) (153) [12,13]	−2.6/−17.3	8.0e−2	9.5e−4	2.0e9	2.4e−4
FDH (364)	−1.7/−14.6	1.9e−3	1.1e−4	1.6e4	3.4e−7

k_f and k_u: rate constant of unimolecular folding and unfolding, respectively.
k_{ass} and k_{diss}: rate constant of bimolecular association and dissociation, respectively.

required good time-resolution in the data and a simultaneous analysis of the progress curves. However, in the analysis of such data, it is interesting to note that summing the individual half-lives for a bi-molecular step ($t_{1/2} = 1/(k_{bi} \times M_o)$) and a unimolecular step ($t_{1/2} = \ln 2 \times k_{uni}$) provides a tolerably close approximation to the overall half-time of refolding. If we use the approximation that the measured $t_{1/2} = 1/(k_{bi} \times M_o) + \ln 2 \times k_{uni}$ then the data sets shown in Fig. 4 can be re-analysed in terms of $t_{1/2}$ versus total monomer concentration. Such a plot is shown in Fig. 5 and the fitting procedure yields a value for k_{bi} of $2.4 \times 10^4\ M^{-1}\ s^{-1}$ and a value for k_{uni} of $1.6 \times 10^{-3}\ s^{-1}$; remarkably close to the values arrived at from global numerical fitting, i.e. $1.6 \times 10^4\ M^{-1}\ s^{-1}$ and $1.9 \times 10^{-3}\ s^{-1}$, respectively. The k_{uni} measured in such reactions might be a compound of two or more unimolecular steps in a more complex mechanism; in this case $1/k_{uni} = \tau_{uni} = \tau_1 + \tau_2 + \cdots \tau_n$.

3.6. Thermal denaturation

Shown in Fig. 6A are denaturation data derived from an experiment in which the enzyme was incubated at a series of temperatures for a period of 20 min and the residual activity recorded. The heat inactivation of *cm*FDH, as for most proteins, is not reversible and follows a first-order decay [21–23]. As a result of this, denaturation cannot be formally treated as an equilibrium system to which the orthodox analysis can be applied, rather it should be thought of as being defined by a temperature-sensitive rate constant for the irreversible step. These data can be treated as representing rate constants of denaturation as a function of temperature, i.e. the rate constant (k) can be derived directly from the residual activity (A) by the following relationship:

$$A = A_o \cdot \exp(-k \cdot t_{inc}) \quad (8)$$

where t_{inc} is the period of incubation (in our case 1200s) and A_o is the initial activity. The variation of rate constant with temperature can be described by the Arrhenius relationship: $k = k_o \cdot \exp(E_a/RT)$ where E_a is the activation enthalpy. When the data in Fig. 6A are fitted to this relationship we obtain a value for k_o of $2 \times 10^{57}\ s^{-1}$ and for E_a a value of 91 kcal/mol.

However, in the knowledge that protein folding involves large changes in heat capacity, it is more realistic to fit the data to the integrated form of the van't Hoff relationship where the free-energy barrier for unfolding is related to temperature by the equation:

$$k = k_o \cdot \exp(-\Delta G/(R \cdot T)) \quad (9)$$

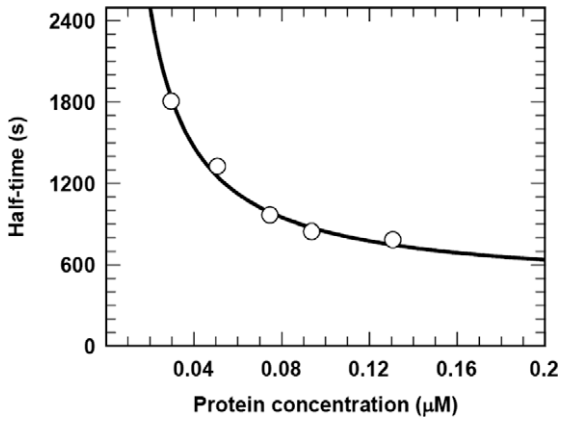

Fig. 5. The relationship between the half-time of refolding and reactant concentration. The refolding half-times were fitted to the equation; $t_{1/2} = 1/(k_{bi} \times M_o) + \ln 2 \times k_{uni}$. The shown fit yields values of $1.6 \times 10^{-3}\ s^{-1}$ and $2.4 \times 10^4\ M^{-1}\ s^{-1}$, respectively, for the unimolecular folding and bimolecular association rate constants.

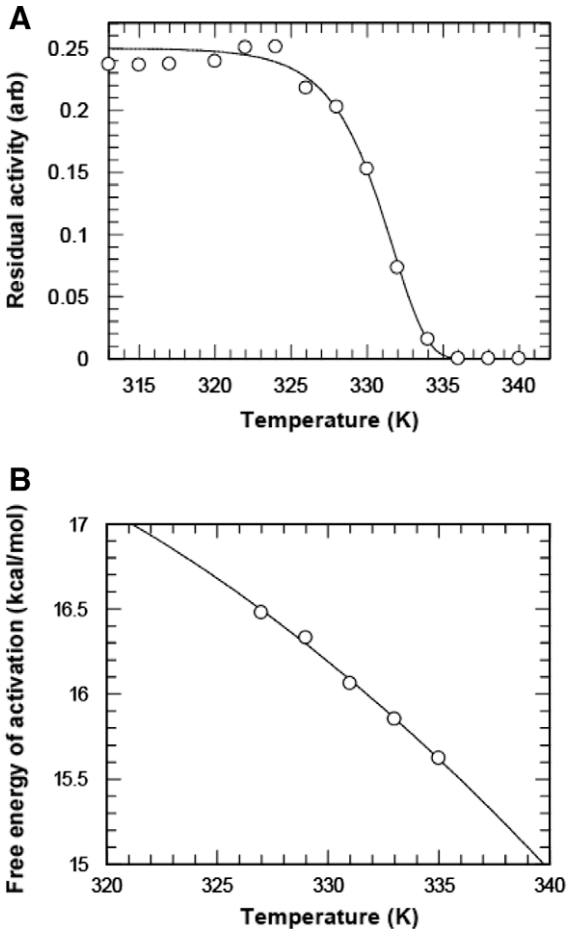

Fig. 6. Heat inactivation of *cm*FDH. (A) The thermal denaturation of *cm*FDH was measured by incubating the enzyme at varying temperatures for 20 min. After this period the residual activity was recorded. The method for fitting the residual activity data is described in Section 2. The plot shown in (B) shows the deduced ΔG for activation against the temperature.

where ΔG is the free energy of activation and k_o is the rate of an unfolding reaction in the absence of an activation barrier. For the purposes of this analysis, we take a value of $10^7\ s^{-1}$ as the upper rate of rearrangements involved in protein folding or unfolding [24].

In Fig. 6B the deduced ΔG for activation is plotted against the temperature. The relationship between the height of the free-energy barrier and the temperature defines the changes in heat capacity, enthalpy and entropy between the folded state and the transition state according to Eq. (2). Combining the above equations allows a direct fit of residual activity against ΔH, ΔC_p and ΔS as shown by the fit line in Fig. 6A which is superimposed on the original data. This analysis gives an enthalpic barrier of 25 kcal/mol, a favourable entropic term (−5.5 kcal/mol at 298 K) and a heat capacity change of 2.0 kcal/mol/K. [Measurements of unfolding rate constants as a function of temperature yielded similar values for ΔH, ΔC_p and ΔS i.e. 31 kcal/mol, 1.6 kcal/mol/K. and −11 kcal/mol at 298 K (see Supplementary Fig. S1)].

Interestingly, these values are comparable to those for the barrier to the unfolding of phosphoglycerate kinase (N-domain) (N-PGK) which shows a favourable entropy term (−6.3 kcal/mol −298 K) and an unfavourable enthalpy (+18.4 kcal/mol) [24]. A further similarity can be seen in the heat capacity change in attaining the transition state in unfolding–folding which in the case of FDH and N-PGK is about 20% of the ΔC_p for complete unfolding, i.e. the transition state is about 80% folded as measured by solvent exposure. It is also intriguing to note that for

chemical denaturation of FDH, according to the Δm-value for the transition state (~4.5, Fig. 3) and the overall Δm value for unfolding (~17.5, Fig. 1), the transition state is about 75% folded. Indeed, using the thermodynamic parameters derived from the rates of thermal denaturation, we would predict the rate of unfolding at 25 °C to be $6 \times 10^{-7}\ s^{-1}$, a value remarkably close to $3 \times 10^{-7}\ s^{-1}$ derived from orthodox denaturant analysis.

Acknowledgements

This work was partially supported by the Turkish State Planning Organization's Advanced Technologies Program and Turkish State Planning Organization (Project No. 90188).

Appendix A. Supplementary data

Supplementary data associated with this article can be found, in the online version, at doi:10.1016/j.febslet.2009.07.048.

References

[1] Rumfeldt, J.A.O., Galvagnion, C., Vassall, K.A. and Meiering, E.M. (2008) Conformational stability and folding mechanisms of dimeric proteins. Progress Biophys. Mol. Biol. 98, 61–84.
[2] Allen, S. and Holbrook, J. (1998) Isolation, sequence and overexpression of the gene encoding NAD-dependent formate dehydrogenase from the methylotrophic yeast *Candida methylica*. Gene 162, 99–104.
[3] Schirwitz, K., Schmidt, A. and Lamzin, V.S. (2007) High-resolution structures of formate dehydrogenase from *Candida boidinii*. Protein Sci. 16, 1146–1156.
[4] Wenfang, L. and Wang, P. (2007) Cofactor regeneration for sustainable enzymatic biosynthesis. Biotechnol. Adv. 25, 369–384.
[5] Tishkov, V.I. and Popov, V.O. (2006) Protein engineering of formate dehydrogenase. Biomol. Eng. 23, 89–110.
[6] Ordu, E.B. and Karagüler, N.G. (2007) Improving the purification of NAD^+ dependent formate dehydrogenase from *Candida methylica*. Prep. Biochem. Biotech. 37, 333–341.
[7] Parker, M.J., Dempsey, C.E., Lorch, M. and Clarke, A.R. (1997) Acquisition of native β-strand topology during the rapid collapse phase of protein folding. Biochemistry 36, 13396–13405.
[8] Kuzmic, P. (1996) Program DYNAFIT for analysis of enzyme kinetic data: application to HIV proteinase. Anal. Biochem. 237, 260–273.
[9] Robertson, A.D. and Murphy, K.P. (1997) Protein structure and the energetics of protein stability. Chem. Rev. 97 (5), 1251–1268.
[10] Mei, G., Venere, A., Rosato, N. and Finazzi-Agro, A. (2005) The importance of being dimeric. FEBS J. 272, 16–27.
[11] Northrup, S.H. and Erıckson, H.P. (1992) Kinetics of protein–protein association explained by Brownian dynamics computer simulation. Proc. Nalt. Acad. Sci. USA, Biochem. 89, 3338–3342.
[12] Zhou, H.X., Wong, K.Y. and Vıjayakumar, M. (1997) Design of fast enzymes by optimizing interaction potential in active site. Proc. Natl. Acad. Sci. USA, Biophys. 94, 12372–12377.
[13] Schlosshauer, M. and Baker, D. (2004) Realistic protein–protein association rates from a simple diffusional model neglecting long-range interactions, free energy barriers, and landscape ruggedness. Protein Sci. 13, 1660–1669.
[14] Schreiber, G. and Fersht, A.R. (1996) Rapid, electrostatically assisted association of proteins. Nat. Struct. Biol. 3 (5), 427–431.
[15] Wallis, R., Leung, K.Y., Osborne, M.J., James, R., Moore, G.R. and Kleanthous, C. (1998) Specificity in protein–protein recognition: conserved Im9 residues are the major determinants of stability in the colicin E9 DNase–Im9 complex. Biochemistry 37 (2), 476–485.
[16] Alsallaq, R. and Zhou, H.X. (2007) Prediction of protein-protein association rates from a transition-state theory. Structure 15 (2), 215–224.
[17] Mallam, A.L. and Jackson, S.E. (2007) A comparison of the folding of two knotted proteins: YbeA and YibK. J. Mol. Biol. 366 (2), 650–665.
[18] Najera, H., Costas, M. and Fernandez-Velasco, D.A. (2003) Thermodynamic characterization of yeast triosephosphate isomerase refolding: insights into the interplay between function and stability as reasons for the oligomeric nature of the enzyme. Biochem. J. 370, 785–792.
[19] Svensson, A.K.E., Bilsel, O., Kondrashkina, E., Zitzewitz, J.A. and Matthews, C.R. (2006) Mapping the folding free energy surface for metal-free human Cu, Zn superoxide dismutase. J. Mol. Biol. 364, 1084–1102.
[20] Vassall, K.A., Stathopulos, P.B., Rumfeldt, J.A.O., Lepock, J.R. and Meiering, E.M. (2006) Equilibrium thermodynamic analysis of amyotrophic lateral sclerosis-associated mutant Apo Cu, Zn superoxide dismutases. Biochemistry 45, 7366–7379.
[21] Sarmentoa, A.C., Oliveiraa, C.S., Pereiraa, A., Esteves, V.I., Moirc, A.J.G., Saraivad, J., Pirese, E. and Barros, M. (2009) Unfolding of cardosin A in organic solvents and detection of intermediaries. J. Mol. Catal. B: Enzym. 57, 115–122.
[22] Rudra, S.G., Shivhare, U.S., Basu, S. and Sarkar, B.C. (2008) Thermal inactivation kinetics of peroxidase in coriander leaves. Food Bioprocess. Technol. 1, 187–195.
[23] Ying, Y. and Zhang, W. (2008) Some properties of polyphenol oxidase from lily. Int. J. Food Sci. Technol. 43 (1), 102–107.
[24] Parker, M.J., Lorch, M., Sessions, R.B. and Clarke, A.R. (1998) Thermodynamic properties of transient intermediates and transition states in the folding of two contrasting protein structures. Biochemistry 37, 2538–2545.